# Iso-entangled bases and joint measurements

Flavio Del Santo [1], Jakub Czartowski [2,3] Karol Życzkowski, [3,4] and Nicolas Gisin [1]

[1] *Group of Applied Physics, University of Geneva, 1211 Geneva 4, Switzerland, and Constructor University, 1205 Geneva, Switzerland*

[2] *Doctoral School of Exact and Natural Sciences, Jagiellonian University, ul. Łojasiewicza 11, 30-348 Kraków, Poland*

[3] *Faculty of Physics, Astronomy and Applied Computer Science, Jagiellonian University, ul. Łojasiewicza 11, 30-348 Kraków, Poland*

[4] *Center of Theoretical Physics, Polish Academy of Sciences, al. Lotników 32/46 02-668 Warszawa, Poland*

(Received 14 July 2023; accepted 16 February 2024; published 23 April 2024)

While entanglement between distant parties has been extensively studied, entangled measurements have received relatively little attention despite their significance in understanding nonlocality and their central role in quantum computation and networks. We present a systematic study of entangled measurements, providing a complete classification of all equivalence classes of iso-entangled bases for projective joint measurements on two qubits. The application of this classification to the triangular network reveals that the elegant joint measurement, along with white noise, is the only measurement resulting in output permutation invariant probability distributions when the nodes are connected by Werner states. The paper concludes with a discussion of partial results in higher dimensions.

DOI: 10.1103/PhysRevResearch.6.023085

## I. INTRODUCTION

In 1935, Schrödinger stated that entanglement is not one but rather *the* characteristic trait of quantum mechanics. Indeed, today it is well-known that entanglement is not only necessary for the violation of celebrated Bell inequalities—disproving local hidden variables—but for most of the applications in quantum information science such as security proofs of quantum cryptography or quantum teleportation, to name but a few examples.

Entanglement is sometimes called the quantum teleportation channel. However, this overlooks the fact that entanglement plays a dual role in this fascinating process: First, as the channel connecting the distant parties, indeed, but also in the joint measurement that triggers the teleportation process [1]. Similarly, these joint measurements are at the heart of entanglement swapping [2] and dense coding [3]. Formally, they are represented in quantum theory by self-adjoint operators which, in turn, are characterized by their eigenvectors. When these eigenvectors are entangled, one says that the measurement is entangled. For example, in the best-known joint measurement, the eigenvectors are the Bell states which are all maximally entangled.

Entanglement between distant parties, traditionally named Alice and Bob, is by now well-studied and understood. However, entangled measurements have so far received relatively little attention [4,5] and, to our knowledge, have never been studied in a systematic manner. This is somewhat surprising and disappointing, given their importance for both the conceptual understanding of quantum foundations and for applications. In fact, it has been recently pointed out that understanding entangled measurements is one of the most interesting future directions in the foundations of quantum physics [6]. Moreover, the problem of joint (entangled) measurements is a central concern for quantum field theory, which, to date, still lacks a complete theory of measurement and faces conceptual issues like the so-called impossible measurements [7,8]. Understanding entangled measurements is necessary to shed light on these fundamental problems [9].

For what concerns the applications, entangled measurements play a major role in quantum computation [10,11], the estimation of coherent states [12] and eigenvalues of channels [13], and in quantum networks [14]. These are pivotal for the development of a quantum internet [15], which is one of the most promising future quantum technologies.

Furthermore, studying entanglement beyond maximal value can lead to deeper understanding and unique applications. Indeed, it is known by now that maximally entangled states are not always the best resource for quantum information tasks: nonmaximally entangled quantum states, in general, outperform maximally entangled ones in most measures of nonlocality, such as Bell inequalities, entanglement simulation with communication, the detection loophole and quantum cryptography [16,17]. While this has not been investigated nearly as thoroughly for joint measurements, it has been shown that nonmaximally entangled measurements represent stronger resources for certain tasks, such as the violation of bilocality [18].

In this paper, we provide the first systematic study of entangled measurements for the simplest case. The problem is known to be difficult in full generality, hence we assume that all the eigenvectors have the same degree of entanglement,

*Published by the American Physical Society under the terms of the Creative Commons Attribution 4.0 International license. Further distribution of this work must maintain attribution to the author(s) and the published article's title, journal citation, and DOI.*

i.e., they form an iso-entangled basis (previous works on non-maximally entangled joint measurements and iso-entangled bases are Refs. [18–24]). Moreover, we mostly limit our analysis to projective joint measurements on two qubits.

Here, we give a complete classification of all iso-entangled bases of two qubits, up to the natural equivalence relation of local unitary rotations and swapping of the qubits. Next, we apply our parametrization to the triangular network and prove that the elegant joint measurement (EJM) (and white noise) is the only measurement that leads to output permutation invariant (OPI) probability distributions when the nodes are connected by identical Werner states. Finally, we discuss partial results in higher dimensions.

## II. COMPLETE CLASSIFICATION OF ALL EQUIVALENCE CLASSES OF ISO-ENTANGLED BASES OF TWO QUBITS

Consider measurements on two qubits, i.e., the partition of the Hilbert space $\mathcal{C}^4 = \mathcal{C}^2 \otimes \mathcal{C}^2$ is fixed. An iso-entangled basis is an orthonormal basis such that all four vectors $|\psi_j\rangle$, $j = 1, \dots 4$, have the same degree of entanglement.

There are many measures of entanglement, but for pure bipartite states $\rho_{AB} = |\psi\rangle\langle\psi|_{AB}$ they are all equivalent [25]. We quantify the degree of entanglement by its *tangle*, equal to squared concurrence [26–28]

$$\xi = 2\big(1 - \mathrm{Tr}\big(\rho_A^2\big)\big) \in [0, 1], \tag{1}$$

where $\rho_A = \mathrm{Tr}_B(\rho_{AB})$ is the reduced density matrix; this monotonically quantifies entanglement from 0 (separable states) to 1 (maximally entangled states).

*Definition 1* (local equivalence of bases). Let us define the equivalence relation $\sim$ : two bases $B_1$ and $B_2$ are equivalent iff they are identical under local unitaries, $U_i$ (equivalently, local changes of basis), or identical under swap $S_{A\leftrightarrow B}$ and local unitaries, i.e.,

$$B_1 \sim B_2 \Leftrightarrow B_2 = (U_A \otimes U_B)(\cdot)B_1 P, \tag{2}$$

with $(\cdot) \in \{\mathbb{1}, S_{A\leftrightarrow B}\}$ and $P$ an arbitrary permutation, corresponding to an arbitrary relabeling of the states within the basis. Our goal is to find a parametrization of each family of equivalence classes. Starting with 12 real parameters for an arbitrary dephased orthonormal basis of $\mathcal{C}^4$ (meaning that for each state $|\psi\rangle$ we disregard the global phase by acknowledging the equivalence of the states within the complex projective space, $|\psi\rangle \sim \frac{\langle\psi|1\rangle}{|\langle\psi|1\rangle|}|\psi\rangle$), we subtract $3+3$ parameters for local changes of bases, and the three constraints that all four vectors have the same degree of entanglement. We thus expect an iso-entangled basis of two qubits to depend, in general, on three parameters.

Our main result consists of the following proposition:

*Proposition 1* (complete classification of iso-entangled bases of two qubits). All equivalence classes of iso-entangled bases on space $C$ with respect to the relation (2) constitute a three-dimensional manifold composed of two families, together with the closure of discontinuous submanifolds, given by three additional families of equivalence classes of smaller dimension. The specific functional form of the families is provided in Eq. (15) for the general family, (12) for the Bell family, and in Eqs. (9) and (10) for the families of smaller dimensions.

*Constructive proof.* Let $B$ be a matrix of order 4 whose columns are four basis vectors $\{|\psi_1\rangle, |\psi_2\rangle, |\psi_3\rangle, |\psi_4\rangle\}$ in $\mathcal{C}^4 = \mathcal{C}^2 \otimes \mathcal{C}^2$. Let us write $B$ in the following skewed basis (by applying local change of basis only), consisting only of product states, but, in general, different from the computational basis,

$$|0, 0\rangle, |0, 1\rangle, |1, \varphi\rangle, |1, \varphi^{\perp}\rangle, \tag{3}$$

where $|\varphi\rangle = \cos(\tau)|0\rangle + \sin(\tau)|1\rangle$ and $|\varphi^{\perp}\rangle = \cos(\tau)|1\rangle - \sin(\tau)|0\rangle$. To simplify the derivation, we use the fact that any two-dimensional subspace of $\mathcal{C}^4$ contains at least one product state [29]. Imposing the orthonormality leads to the following parametrization of an arbitrary equivalence class of two-qubit orthonormal bases (for derivation, see Appendix A):

$$B_{|\varphi\rangle} = \begin{pmatrix} 0 & 0 & -c\alpha\cdot e^{i\gamma} & s\alpha\cdot e^{i\gamma} \\ s\delta\cdot c\theta & c\delta\cdot c\theta & -s\alpha\cdot s\theta & -c\alpha\cdot s\theta \\ s\delta\cdot s\theta & c\delta\cdot s\theta & s\alpha\cdot c\theta & c\alpha\cdot c\theta \\ -c\delta\cdot e^{i\beta} & s\delta\cdot e^{i\beta} & 0 & 0 \end{pmatrix}, \tag{4}$$

where we have introduced the compact notation $c\delta = \cos\delta$, $s\delta = \sin\delta$, and similarly for $c\alpha$ and $s\alpha$, and $c\theta$ and $s\theta$. The subscript $|\varphi\rangle$ indicates that the coefficients are expressed in the basis provided in Eq. (3). As expected, this parametrization has 6six parameters: $\alpha, \delta, \theta, \gamma, \beta$, and $\tau$ [with $\tau$ included implicitly in skewed basis (3)].

By computing the tangle $\xi_j$ [Eq. (1)] for each state $|\psi_j\rangle$ of $B$, we can now impose the constraints of iso-entanglement:

$$\xi_i = \xi_j, \quad \forall i, j \in \{1, 2, 3, 4\}. \tag{5}$$

Note that only three of these equations are independent; thus, solving these constraints will lead to a parametrization depending on $6-3=3$ parameters. The previous equations yield the following complete set of solutions:

(i) $\cos\theta = 0$, or
(ii) $\sin 2\theta \neq 0$, and $\sin\tau = 0 \Rightarrow \alpha = \frac{\pi}{4} = \pm\delta + \frac{l\pi}{2}$, or
(iii.a) $\sin\theta = 0$, and $\sin\tau \neq 0 \Rightarrow \alpha = \pm\delta + \frac{k\pi}{2}$, or
(iii.b) $\cos\tau = 0 \Rightarrow \alpha = \pm\delta + \frac{m\pi}{2}$, or
(iv) $\cos\theta \neq 0$, and $\sin\theta \neq 0$, and $\cos\tau \neq 0$, and $\sin\tau \neq 0$, and $\sin(2\delta) \neq 0$, and $\sin(2\alpha) \neq 0 \Rightarrow \alpha = \pm\delta + \frac{n\pi}{2}$.

As we shall see, the first solution ($\cos\theta = 0$) is somehow trivial, for it leads to all four basis states being separable. All the other solutions imply that $\alpha = \pm\delta$ (omitting here the periodicity of $\pi/2$). This condition can thus be substituted in (three of) Eq. (5), leading to the following simplified expressions for the iso-entanglement conditions:

$$0 = \xi_1 - \xi_2 = -8\cos^2\theta\sin\theta\cos\tau \cdot (\cos\tau\sin\theta\cos(2\delta) - \sin\tau\sin(2\delta)\cos\beta), \tag{6}$$

$$0 = \xi_3 - \xi_4 = -8\cos^2\theta\sin\theta\cos\tau \cdot (\cos\tau\sin\theta\cos(2\delta) + \sin\tau\sin(2\delta)\cos\gamma), \tag{7}$$

$$0 = \xi_1 - \xi_3 = 8\cos^2\theta\sin\theta\cos\tau \cdot \sin(2\delta)\sin^2\delta\sin\tau(\cos\beta + \cos\gamma). \tag{8}$$

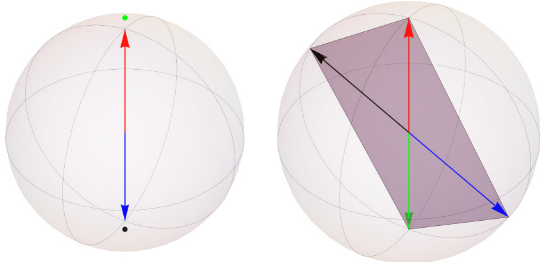

FIG. 1. Both reduction density matrices for four pure states for an exemplary member of the skewed product family. Note that in the first reduction (left), all states lie on the $z$ axis, while in the second they form a rectangle in the $x$-$z$ plane.

We are now in a position to fully characterize the different classes of parametrizations of iso-entangled bases of two qubits. These correspond to the five different solutions (i)–(v) above of Eqs. (6)–(8). Note, however, that two of the solutions [namely, (iii.a) and (iii.b)], lead to equivalent families up to a swap (so they belong to the same equivalence class). Therefore, we arrive at four families of iso-entangled bases. We will denominate the different families $I^{(j)}$ with $j \in (1, \dots, 4)$, and we will express them in either the computational basis or in the skewed basis (3); we will indicate this by a subscript $|0\rangle$ or $|\varphi\rangle$, respectively. We will see that each of them is characterized not only by a different functional form of the states (which reflects different geometrical properties thereof) but also by the amount of parameters which the degree of entanglement $\xi^{(j)}$ depends on.

## III. FOUR INEQUIVALENT FAMILIES OF ISO-ENTANGLED BASES

Solutions (i)–(iv) lead to the following four families of isoentangled bases:

*1. Skewed product family*. Starting from condition (i), the parametrization can be reduced to

$$I^{(1)}_{|0\rangle} = \begin{pmatrix} 1 & 0 & 0 & 0 \\ 0 & 1 & 0 & 0 \\ 0 & 0 & \cos\tau & -\sin\tau \\ 0 & 0 & \sin\tau & \cos\tau \end{pmatrix}, \tag{9}$$

where the other parameters have been absorbed into local transformations. Note that the degree of entanglement is $\xi^{(1)} = 0$, independently of $\tau$. As already mentioned, this family contains only product bases, equivalent to the skewed basis provided in Eq. (3).

From the point of view of the Bloch ball (see Fig. 1), this family is always composed from two twice degenerate points on the north and south poles in one reduction, and two pairs of opposite poles in the other.

*2. Elegant family.* Condition (ii) yields a family which can be parametrized as

$$I^{(2)}_{|0\rangle} = \frac{1}{\sqrt{2}} \begin{pmatrix} 0 & 0 & -e^{i\zeta} & e^{i\zeta} \\ c\theta & c\theta & -s\theta & -s\theta \\ s\theta & s\theta & c\theta & c\theta \\ 1 & -1 & 0 & 0 \end{pmatrix}, \tag{10}$$

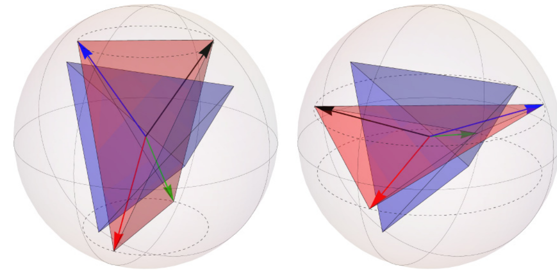

FIG. 2. Partial traces for a selected member of the elegant family (in red) together with the EJM (blue). A generic member of this family forms simplex structures with all states lying on cones with opening angles $2\theta$ and $\pi - 2\theta$ for the two reductions, respectively; the second pair is rotated with respect to the first by an angle $\zeta$. In particular, EJM is found by setting $\theta = \pi/4$ and $\zeta = \pi/2$, thus forming two regular simplices.

where we have introduced the local transformation of the form $\exp(i\zeta\sigma_z)^{\otimes 2}$, with $\zeta = \gamma - \beta$. Hence, this family has only two parameters. Note that in this case, the skewed basis and the computational one correspond, i.e., $|\varphi\rangle = |0\rangle$. The squared concurrence reads

$$\xi^{(2)} = \frac{\sin^2(2\theta)}{4}, \tag{11}$$

which depends only on one parameter. Note that the degree of entanglement is bound: $\xi^{(2)} \in [0, \frac{1}{4}]$. Nil entanglement (i.e., $\xi^{(2)} = 0$) corresponds to $\theta = 0$, which leads again to the separable basis (3). The maximal amount of entanglement, $\xi^{(2)} = 1/4$, is obtained by $\theta = \pi/4$. Note that this family contains the EJM, which plays a special role in network nonlocality [30]. EJM has, in fact, $\xi = 1/4$, and is retrieved for $\zeta = \pi/2$. Since EJM is the extremal case of this family, we name this the elegant family. Fixing the maximal amount of entanglement, however, does not single out EJM and leads to a one-parameter subfamily.

In Bloch ball representation (see Fig. 2), the first two states lie on a hyperbole in the $x$-$z$ plane, whereas the other two lie on a full rotational hyperboloid with symmetry around the $z$ axis. The opening angle of the limiting cone of these hyperboloids is $\theta$ in one, and $\pi - \theta$ in the other reduction. A generic member of this family forms a simplex with three pairs of edges of different lengths. The EJM is singled out by maximizing the volume of both reductions.

*3. Bell family.* This family is the conflation of conditions (iii.a) and (iii.b), which are equivalent up to a swap $S_{A\leftrightarrow B}$ and substituting $\tau$ by $\theta$, respectively. In both cases, phase $e^{i\beta}$ can be reabsorbed into the computational state $|1\rangle$ of the first qubit and defining $\zeta = \gamma + \beta$, or into $|0\rangle$ of the second qubit and defining $\zeta' = \gamma - \beta$, respectively. Hence, this family reads

$$I^{(3)}_{|0\rangle} = \begin{pmatrix} 0 & 0 & -c\delta \cdot e^{i\zeta} & s\delta \cdot e^{i\zeta} \\ s\delta & c\delta & 0 & 0 \\ s\tau \cdot c\delta & -s\tau \cdot s\delta & c\tau \cdot s\delta & c\tau \cdot c\delta \\ -c\tau \cdot c\delta & c\tau \cdot s\delta & s\tau \cdot s\delta & s\tau \cdot c\delta \end{pmatrix}. \tag{12}$$

Hence, one has the three expected parameters ($\delta$, $\zeta$, and $\tau$). The tangle reads

$$\xi^{(3)} = \sin^2(2\delta)\sin^2(\tau), \tag{13}$$

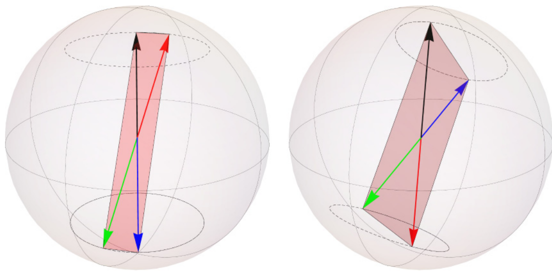

FIG. 3. Generic member of the Bell family. Note that the four vectors in both reductions form two rectangles, with the first one lying on a cone with the rotation axis along the $z$ axis.

which depends on two parameters and varies between 0 and 1. For $\delta = \pi/4$ and $\tau = \pi/2$, one achieves maximally entangled states, i.e., $\xi^{(3)} = 1$. This is equivalent to the standard *Bell state measurement*, which is the unique maximally entangled basis up to local transformations [31]. This thus suggests the name of this family. For nil entanglement, i.e., $\xi^{(3)} = 0$, one has either $\delta = 0$, or $\cos(\tau) = \pm 1$; both cases are equivalent to the already discussed separable family (3).

Despite the full range of attainable entanglement, from the perspective of the Bloch ball, this family always produces rectangles lying in the $x$-$z$ plane in one reduction, and in a rotated plane in the other, with rotation being controlled by the $\zeta$ phase. In particular, we note that in Bloch representation (see Fig. 3), a part of the Bell family will overlap with the subset of the elegant family with $\zeta = 0$.

An alternative derivation of this family, resulting in a canonical form, is given in Appendix B.

*4. General family.* In the case of condition (iv), we find that, necessarily, we have $e^{i\gamma} = -e^{\pm i\beta}$, which yields the relation

$$\tan(\tau) = \frac{\cos(2\delta)\sin(\theta)}{\sin(2\delta)\cos(\beta)}. \tag{14}$$

Hence, the parametrization reads

$$I^{(4)}_{|\varphi\rangle} = \begin{pmatrix} 0 & 0 & c\delta \cdot e^{\pm i\beta} & -s\delta \cdot e^{\pm i\beta} \\ s\delta \cdot c\theta & c\delta \cdot c\theta & -s\delta \cdot s\theta & -c\delta \cdot s\theta \\ s\delta \cdot s\theta & c\delta \cdot s\theta & s\delta \cdot c\theta & c\delta \cdot c\theta \\ -c\delta \cdot e^{i\beta} & s\delta \cdot e^{i\beta} & 0 & 0 \end{pmatrix}. \tag{15}$$

The expected three parameters are $\delta, \theta$, and $\beta$. The tangle reads

$$\xi^{(4)} = \frac{\sin^2(2\theta)\sin^2(2\delta)}{4} \cdot \frac{\sin^2(2\delta)\cos^2(\beta) + \cos^2(2\delta)}{\sin^2(2\delta)\cos^2(\beta) + \cos^2(2\delta)\sin^2(\theta)}, \tag{16}$$

which varies between 0 and 1. Note that this is the most general family of iso-entangled bases, for its degree of entanglement depends on all three parameters and has overlaps with all the other families. Furthermore, a generic basis from this family will yield nondegenerate simplices in both reductions.

Note that Eqs. (14) and (16) have five singularity points. Studying the (directional) limits of these multivariable functions yields the following cases:

(i) $\lim \beta \to \pi/2$ reduces the general family (15) to a two-parameter subfamily of the Bell family (12). In particular, this implies that $\tau \to \pi/2$ and $\xi^{(4)} \to \cos^2(\theta)\sin^2(2\delta)$, which has the same form of Eq. (13). Note that the Bell family depends on the same number of parameters as the general family, therefore it cannot be fully retrieved by any of the limits.

(ii) $\lim \delta \to \pi/4$ reduces the general family to the elegant family (10).

(iii) $\lim \theta \to 0$ and $\delta \to 0$ reduces the general family to the skewed product family (9), independently of the direction of approach of these limits.

(iv) $\lim \beta \to \pi/2$ and $\delta \to \pi/4$ lead to an interpolation between a part of the elegant family and a subfamily of the Bell family, depending on the direction of approach of the limit. In Ref. [18], a one-parameter iso-entangled family was proposed that also interpolates between EJM and BSM. However, this cannot be contained within this limit case because the latter does not admit regular simplices within the reductions, contrarily to the family in Ref. [18] (see Appendix C).

(v) $\lim \beta \to \pi/2$ and $\lim \theta \to 0$ leads to a subfamily of the Bell family wherein, however, the degree of entanglement is upper bounded, with the bound depending on the angle of approach $\phi \in (-\pi/2, \pi/2)$ as $(1 + \tan(|\phi|))^{-2}$.

From this, one sees that the three particular families (9), (10), and (12) (partly) form the closure of the General family.

### A. An application to quantum networks

Let us consider a triangular network scenario, in which Alice, Bob, and Charlie share pairwise a Bell state of two qubits, e.g.,

$$|\Psi\rangle_{ABC} = |\psi_+\rangle_{AB} \otimes |\psi_+\rangle_{AC} \otimes |\psi_+\rangle_{BC}, \tag{17}$$

with $\psi_+ = \frac{1}{\sqrt{2}}(|00\rangle + |11\rangle)$, and each chooses a basis to perform a joint measurement on their pair of qubits (see Ref. [32]). The scenario is said to be OPI if the output probability distribution can be defined by three constants

$$p_1 = p_{iii}, \quad p_2 = p_{\sigma(iij)}, \quad p_3 = p_{\sigma(ijk)} \tag{18}$$

for $i \neq j$, $j \neq k$, $k \neq i$ and any permutation $\sigma$; intuitively, it means that no node, nor output, of the network is distinguished. A similar notion can be defined for larger networks based on the network graph automorphism group.

Since the iso-entangled bases set each of the measurement states on equal footing, they appear to be natural candidates for measurements realizing OPI in such networks. We find that setting $\zeta = \pi/2 + \arccos(-\sin(2\theta))$ followed by the local transformation $\exp(-\frac{i}{4}\arccos(-\sin(2\theta))\sigma_z)^{\otimes 2}$ in the elegant family leads to a one-parameter subset of measurements, which leads to OPI distributions. Interestingly, none of the measurements in this family, except for the extremal points, remains OPI under local noise $\Phi_\epsilon(\rho) = (1-\epsilon)\rho + \frac{\epsilon}{4}\mathbb{I}$ acting on each edge of the network (see Fig. 4).

## IV. DISCUSSION AND OUTLOOK

In this paper, we have provided complete classification of all the equivalence classes of bases of two qubits, whose four states have all the same degree of entanglement (i.e., iso-entangled bases). In particular, we have shown that there exist four inequivalent families of equivalence classes,

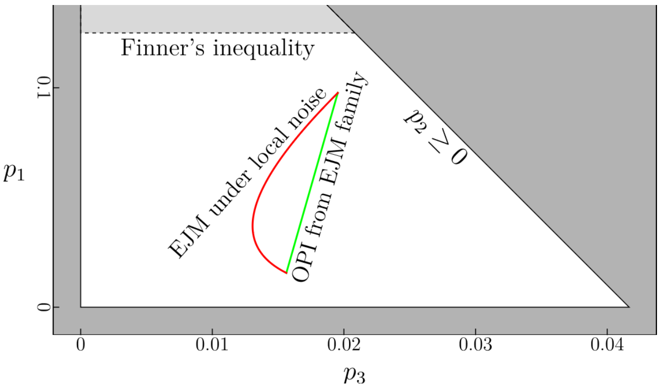


FIG. 4. $p_3$-$p_1$ plane for OPI measurements, with the red line representing probabilities corresponding to EJM acting on Bell states under local noise, $\Phi_\epsilon(|\psi_+\rangle\langle\psi_+|)^{\otimes 3}$, while green line corresponds to the OPI stemming from the elegant family acting on the network state $|\Psi\rangle\langle\Psi|$ from (17). The Finner inequality is known to be a bound for local and quantum distributions [33].

characterized by their numbers of parameters and geometrical constraints of their reductions in the Bloch ball representation.

This paper represents a necessary step towards a deeper understanding of entangled measurements, a topic that has received surprisingly little attention—especially if compared to entangled states between distant parties—despite their pivotal importance for our fundamental understanding of measurements in different quantum frameworks (including quantum field theory) and in applications such as quantum computation, and other quantum tasks (quantum teleportation, dense coding, nonlocality in networks, etc.).

Although our findings provide the theoretical framework for further studies, many questions remain open. Most of the aforementioned tasks, such as quantum teleportation or dense coding, make use of Bell state measurements. Our paper provides a tool to start asking in a systematic manner questions like: For which tasks do partially entangled measurements provide stronger resource than the maximally entangled ones? This can bring insights into nonlocality, especially in the context of quantum networks with no inputs, in which nonlocality is triggered exclusively by the selected measurements. Moreover, further questions arise concerning implementability: Which of the entangled measurements can be experimentally realised using standard resources such as linear optical elements?

Furthermore, this preliminary study has addressed only the problem of entangled measurements in the simplest case of two qubits. The natural extension to higher dimensions turns out to be hard, with sparse known examples in literature [20–22,34]. In Appendix D, we provide a short review of already known families together with another family of partially entangled bases. This represents an attempt towards a generalization to higher dimensions that will remain a direction of future research.

## ACKNOWLEDGMENTS

We thank O. Gühne for pointing out Ref. [29] to us. F.D.S. acknowledges support from FWF (Austrian Science Fund) through an Erwin Schrödinger Fellowship (Project No. J 4699s). J.Cz. and K.Ż. gratefully acknowledge financial support by Narodowe Centrum Nauki under the Quantera Projects No. 2021/03/Y/ST2/00193 and No. 2019/35/O/ST2/01049. The research has also been supported by a grant from the Priority Research Area DigiWorld under the Strategic Programme Excellence Initiative at Jagiellonian University. N.G. acknowledges support from the Swiss National Science Foundation via the NCCR-SwissMap.

## APPENDIX A: CANONICAL LOCAL FORM OF THE BASIS

Let us denote with $B$ the matrix whose columns are the vectors $\{|\psi_1\rangle, |\psi_2\rangle, |\psi_3\rangle, |\psi_4\rangle\}$ with coefficients expressed in the computational basis. Any two-dimensional subspace spanned by, e.g., $|\psi_3\rangle$ and $|\psi_4\rangle$, necessarily contains (at least) one product state (Theorem 2 in Ref. [29]). We may introduce local rotations in such a way that it corresponds to the state $|0,0\rangle$. Hence, the first line of the matrix representing that basis starts with two zeros. Similarly, the subspace spanned by $|\psi_1\rangle$ and $|\psi_2\rangle$ contains a product state $|\vartheta,\varphi\rangle$ which is necessarily orthogonal to $|0,0\rangle$. Without loss of generality, let us assume $|\vartheta\rangle = |1\rangle$, whereas $|\varphi\rangle = \cos(\tau)|0\rangle + \sin(\tau)|1\rangle$ and $|\varphi^\perp\rangle = \cos(\tau)|1\rangle - \sin(\tau)|0\rangle$. Hence, one gets $\psi_{33}\cdot\psi_{44} = \psi_{34}\cdot\psi_{43}$, where $\psi_{jk} = \chi_{jk}e^{i\phi_{jk}}$ denotes the element $j,k$ of the matrix $B$, i.e., the $k$th component of vector $|\psi_j\rangle$ in the computational basis. Next, we choose the phases of $\psi_3$ and $\psi_4$ such that their fourth components are real, i.e., $\psi_{34} = \chi_{34}$ and $\psi_{44} = \chi_{44}$. The aforementioned relation implies that $\phi_{33} = \phi_{43} := \phi$. Thus, it is possible to remove this phase by applying the local transformation of the form $\exp(i(\sigma_z\otimes\mathbb{1} - \mathbb{1}\otimes\sigma_z)\phi)$. Hence, the general form of our basis written in the computational basis is given by

$$B_{|0\rangle} = \begin{pmatrix} 0 & 0 & \cdot & \cdot \\ \cdot & \cdot & \cdot & \cdot \\ \cdot & \cdot & \chi_{33} & \chi_{43} \\ \cdot & \cdot & \chi_{34} & \chi_{44} \end{pmatrix}, \tag{A1}$$

where the four displayed entries are real and satisfy the relation $\chi_{33}\cdot\chi_{44} = \chi_{34}\cdot\chi_{43}$.

Let us now write B in the skewed basis provided in Eq. (3). This implies that the last two entries of the last line are also zeros. Starting from the form of the basis provided in Eq. (19), let us choose the global phases such that the third component of each vector is real, i.e., $\psi_{k3} = \chi_{k3}$. Applying the local change of basis in Eq. (3) leads to

$$B_{|\varphi\rangle} = \begin{pmatrix} 0 & 0 & \psi_{31} & \psi_{41} \\ \psi_{12} & \psi_{22} & \psi_{32} & \psi_{42} \\ \chi_{13} & \chi_{23} & \chi_{33} & \chi_{43} \\ \psi_{14} & \psi_{24} & 0 & 0 \end{pmatrix}. \tag{A2}$$

These coefficients depend at this point, in general, on 20 real parameters (21 counting also $\tau$ in the definition of the skewed basis).

We now impose the orthogonality constraints between the pair of vectors for which two components of the scalar product vanish. Denoting by $\chi_{jk}$ the norm of each (in general, complex) element $\psi_{jk}$, from $\langle\psi_1|\psi_3\rangle$ it follows that

$\chi_{12} \cdot \chi_{32} = \pm\chi_{13} \cdot \chi_{33}$ and $\phi_{12} = \phi_{22}(+k\pi)$; from $\langle\psi_2|\psi_3\rangle$, that $\chi_{22}\cdot\chi_{32} = \pm\chi_{23}\cdot\chi_{33}$ and $\phi_{22} = \phi_{32}(+l\pi)$; from $\langle\psi_1|\psi_4\rangle$, that $\chi_{12} \cdot \chi_{42} = \pm\chi_{13} \cdot \chi_{43}$ and $\phi_{12} = \phi_{42}(+m\pi)$; and, finally, from $\langle\psi_2|\psi_4\rangle$, one finds that $\chi_{22} \cdot \chi_{42} = \pm\chi_{23} \cdot \chi_{43}$ and $\phi_{22} = \phi_{42}(+n\pi)$.

In the next step, we reintroduce the normalization constraints. Note that since in the considered skewed basis, each vector has only three nonzero components, such that the normalization can be written as $|\psi_j|^2 = a_j^2 + b_j^2 + c_j^2$, where each $a_j, b_j, c_j$ is one of the nonzero real component $\chi_{jk}$ of the $j$th vector. Note that imposing the normalization conditions $|\psi_j|^2 = 1$ leads to the following general parametrization:

$$\begin{aligned} a_j &= \sin(\alpha_j)\sin(\beta_j),\\ b_j &= \sin(\alpha_j)\cos(\beta_j),\\ c_j &= \cos(\alpha_j). \end{aligned}$$

This, together with the four orthogonality conditions above, leads to reduce the matrix of coefficients to eight real parameters (nine, also counting also $\tau$ in the definition of the skewed basis). After this simplification, we impose the orthogonality constraints of the last two pair of vectors $\langle\psi_1|\psi_2\rangle$, and $\langle\psi_3|\psi_4\rangle$, which remove two additional parameters. Finally, one can apply a further local rotation that eliminates one last parameter, leading to the form in Eq. (4) which depends, as anticipated, on five explicit parameters (six if one counts also the implicit $\tau$).

## APPENDIX B: CANONICAL FORM OF THE BELL FAMILY

Here we provide a canonical form of the Bell family by starting from its geometric structure, which will allow us to give the three free parameters explicit interpretations. We start by defining local bases

$$\begin{aligned} &|A_1\rangle = \cos x|0\rangle + \sin x|1\rangle \quad |A_2\rangle = \cos x|0\rangle - \sin x|1\rangle,\\ &|B_1\rangle = \cos y|0\rangle + \sin y|1\rangle \quad |B_2\rangle = \cos y|0\rangle - \sin y|1\rangle, \end{aligned} \tag{B1}$$

together with the orthogonal states marked by the upper index, $|\cdot^{\perp}\rangle$, defined such that the second entry is dephased. Then, we define the four bipartite states in the basis as

$$\begin{aligned} |\psi_1\rangle &= \cos z|A_1\rangle|B_1\rangle + e^{i\phi_1}\sin z|A_1^{\perp}\rangle|B_1^{\perp}\rangle,\\ |\psi_2\rangle &= \cos z|A_1^{\perp}\rangle|B_2\rangle + e^{i\phi_2}\sin z|A_1\rangle|B_2^{\perp}\rangle,\\ |\psi_3\rangle &= \cos z|A_2\rangle|B_1^{\perp}\rangle + e^{i\phi_3}\sin z|A_2^{\perp}\rangle|B_1\rangle,\\ |\psi_4\rangle &= \cos z|A_2^{\perp}\rangle|B_2^{\perp}\rangle + e^{i\phi_4}\sin z|A_2\rangle|B_2\rangle, \end{aligned} \tag{B2}$$

with $z \in [0, \pi/4]$. These four states follow the general geometric property of the Bell family considered in the Bloch ball: In both reductions, there are two pairs of colinear states, and if a pair is colinear in reduction $A$, it is not colinear in reduction $B$.

To derive generic member of the Bell family, we impose that $\sin x \neq 0$ and analogically for cosines and $y$ variable. After carrying out elementary inner products between the states, we find that the phases are given by

$$\phi_1 = -\phi_2 = -\phi_3 = \phi_4 \tag{B3}$$

and

$$\cos(\pm\phi_1) = -\frac{\tan 2x \tan 2y}{\sin 2z}. \tag{B4}$$

In this way, we arrive at the canonical form for the Bell family, since the three parameters are well connected to the properties of the resulting bases: $x$ and $y$ angles are connected to the geometric arrangement in the Bloch ball, while $z$ angle corresponds to the degree of entanglement in the basis.

## APPENDIX C: PLACING FAMILY FROM REF. [18] WITHIN THE GENERAL FAMILY

A family of iso-entangled bases, $I^{(5)} = \{|\psi_i\rangle\}_{i=1}^4$, has been considered in Ref. [18] in the context of violating bilocality in a linear three-partite network. It can be given explicitly in the form

$$I^{(5)}_{|0\rangle} = \frac{1}{2\sqrt{2}}\begin{pmatrix} 1+i & 1-i & 1-i & 1+i\\ -ie^{i\phi}-i & ie^{i\phi}-i & i-ie^{i\phi} & ie^{i\phi}+i\\ ie^{i\phi}-i & -ie^{i\phi}-i & ie^{i\phi}+i & i-ie^{i\phi}\\ 1-i & 1+i & 1+i & 1-i \end{pmatrix}, \tag{C1}$$

which, *a priori*, does not correspond to any of the families introduced in this paper. By considering the simple fact that it interpolates between EJM and Bell state measurements for $\phi = 0$ and $\phi = \frac{\pi}{2}$, it cannot lie in the skewed-product family, Bell family, or elegant family—therefore, it is natural to assume it to be fully embeddable within the general family.

To find its relation to the members of the general family, let us first define $v_i^A$ as the Bloch vector corresponding to the $A$ reduction of the state $|\psi_i\rangle$, and likewise for $B$ reduction. We will consider the Gram matrices

$$(G_A)_{ij} = v_i^A \cdot v_j^A, \quad (G_B)_{ij} = v_i^B \cdot v_j^B. \tag{C2}$$

Similarly, we define $\tilde{G}_A$ and $\tilde{G}_B$ for members of the general family $I^{(4)} = \{|\tilde{\psi}_i\rangle\}_{i=1}^4$. Using the above, we define a cost function

$$F(\beta,\ \theta,\ \delta) = \sum_{i,j}\left(G_{ij}^A - \tilde{G}^A_{\sigma(i)\sigma(j)}\right)^2 + \left(G_{ij}^B - \tilde{G}^B_{\sigma(i)\sigma(j)}\right)^2, \tag{C3}$$

and we use minimization of the above function with respect to the parameters $\beta,\ \theta,\ \delta$ with the acceptance threshold of $F \leqslant \epsilon = 10^{-12}$. Using this, we arrive numerically at curves $(\beta(\phi),\ \theta(\phi),\ \delta(\phi))$ for embedding the family $I^{(5)}_{|0\rangle}$ within the general family, as shown in Fig. 5.

## APPENDIX D: PROBABILITIES AND NOISE IN A TRIANGULAR NETWORK

Let us consider three parties—Alice, Bob, and Charlie—sharing a joint state of six qubits, a pair per party. Each pair is initialized in the maximally entangled state $|\Psi_+\rangle = (|0,0\rangle + |1,1\rangle)/\sqrt{2}$ (see Fig. 6). Thus, the overall network state without noise is given by

$$|\Psi\rangle_{ABC} = |\psi_+\rangle_{AB} \otimes |\psi_+\rangle_{BC} \otimes |\psi_+\rangle_{AC}. \tag{D1}$$

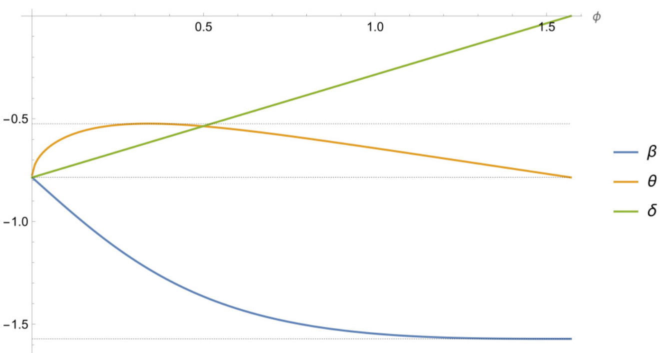


FIG. 5. Family of iso-entangled bases defined in (C1) can be placed within the general family as defined in (15) (in the main text) using numerically generated functions $\beta(\phi)$, $\theta(\phi)$, and $\delta(\phi)$, with the last one expressible directly as $\delta = (\phi - \pi/2)/2$.

The measurement of the network state is carried out by implementing the same local von Neumann measurement $\mathbb{M}$ defined by a selected basis $B = \{|\phi_i\rangle\}_{i=1}^4$. The probability of Alice, Bob, and Charlie outputting results $i$, $j$, and $k$, respectively, is then given by

$$p_{ijk} = \left|\langle\Phi_{ijk}|\Psi\rangle_{ABC}\right|^2 = \mathrm{Tr}(|\Phi_{ijk}\rangle\langle\Phi_{ijk}||\Psi\rangle\langle\Psi|), \quad \text{(D2)}$$

where we define $|\Phi_{ijk}\rangle = |\phi_i\rangle \otimes |\phi_j\rangle \otimes |\phi_k\rangle$ for convenience. OPI distribution is characterized by just three numbers,

$$p_1 = p_{iii}, \quad p_2 = p_{\sigma(iij)}, \quad p_3 = p_{\sigma(ijk)}, \quad \text{(D3)}$$

with $i \neq j \neq k$ and $\sigma$ any permutation on three elements. The name OPI stems from the fact that for such distributions, any permutation of the three involved parties leaves the output probability unchanged.

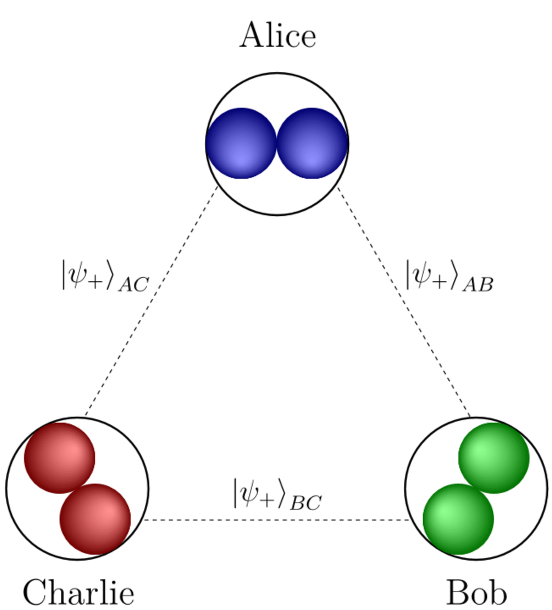


FIG. 6. Triangular network, where three parties—Alice, Bob, and Charlie—share a distributed network state. We assume that each pair shares a maximally entangled state of qubits, $|\psi_+\rangle = (|00\rangle + |11\rangle)/\sqrt{2}$.

By evaluating the outcome probabilities for measurement bases $B$ coming from our families $I^{(1)}$ through $I^{(4)}$ we find that, except for the expected solutions stemming from certain local bases, maximally entangled Bell bases, and the EJM, a subfamily contained in $I^{(4)}$ which generates a one-parameter set of OPI distributions in the triangular network. We find it by setting the phase $\zeta = \pi/2 + \arccos(-\sin(2\theta))$ and introducing a local rotation of the form $\exp(-\frac{i}{4}\arccos(-\sin(2\theta))\sigma_z)^{\otimes 2}$. The resulting OPI distribution with

$$p_1 = \frac{29 - 21x}{512}, \quad p_2 = \frac{3x + 5}{512}, \quad p_3 = \frac{9 - x}{512}, \quad \text{(D4)}$$

with $x = \cos(4\phi)$ interpolates linearly between the distribution generated by EJM and a flat distribution (see green line in Fig. 4), which can be generated with a local measurement. Furthermore, the entire family of the OPI distributions above remains OPI under global noise channel $\Xi$ of the form

$$\Xi(|\Psi\rangle\langle\Psi|)_\delta = (1 - \delta)|\Psi\rangle\langle\Psi| + \delta\frac{\mathbb{I}}{64}. \quad \text{(D5)}$$

Interestingly, however, for $0 < \phi < \frac{\pi}{4}$ the measurements belonging to the discussed sub-family cease to generate OPI distributions under the action of local noise, which transforms the input network state into

$$[\Phi_\epsilon(|\psi\rangle\langle\psi|)]^{\otimes 3} = \left((1 - \epsilon)|\psi_+\rangle\langle\psi_+| + \epsilon\frac{\mathbb{I}}{4}\right)^{\otimes 3}. \quad \text{(D6)}$$

The trivial exception of $\phi = 0$ is the case of local measurements with local noises, and as such can be expected to remain a flat distribution with $p_1 = p_2 = p_3 = 1/64$. More interestingly, the $\phi = \pi/4$ case, equivalent to the EJM,

$$B = \frac{1}{2}\begin{pmatrix} 0 & 0 & -i\sqrt{2} & i\sqrt{2} \\ 1 & 1 & -1 & -1 \\ 1 & 1 & 1 & 1 \\ \sqrt{2} & -\sqrt{2} & 0 & 0 \end{pmatrix}, \quad \text{(D7)}$$

leads to the following OPI distribution:

$$\begin{aligned} p_1 &= \frac{-3\epsilon^3 + 18\epsilon^2 - 36\epsilon + 25}{256}, \\ p_2 &= \frac{\epsilon^3 - 6\epsilon^2 + 8\epsilon + 1}{256}, \\ p_3 &= \frac{-\epsilon^3 + 6\epsilon^2 - 6\epsilon + 5}{256}, \end{aligned} \quad \text{(D8)}$$

which is depicted as the red line in Fig. 4. Thus, we find two one-parameter families of OPI distributions which are joined only at their extreme points. Using extensive numerical searches, we have not been able to generate any other OPI distributions, which leads us to conjecture that these are the only possible cases for a triangular quantum network.

## APPENDIX E: ISOENTANGLED FAMILIES IN HIGHER DIMENSIONS

The natural next step after the analysis of the simplest two-qubit bases is to shift to objects with larger local dimension, residing in spaces $\mathcal{C}^d \otimes \mathcal{C}^d$. Direct application of methods presented in this paper does not seem to be realistic, thus we expect that new techniques would need to be developed to extend the current results beyond qubits. Nevertheless, there exist certain partial results and limited families in the literature.

Separable bases are the simplest case, and can be fully given in terms of *conditional measurement bases*

$$|\psi_{ij}\rangle = |i\rangle \otimes |j_i\rangle, \tag{E1}$$

where one imposes the relations

$$\langle i|i'\rangle = \delta_{ii'}, \quad \langle j_i|j_{i'}\rangle = \delta_{jj'}. \tag{E2}$$

and the product of the form $\langle j_i|j'_{i'}\rangle$ need not be defined for $i \neq i'$. Using local transformations, we can always set the local bases $|i\rangle$ and $|j_0\rangle$ to the computational basis, thus simplifying this family to a direct sum of unitaries, $\sum_{i=1}^{d} U_i$.

The other extreme—bases composed of maximally entangled states—have been considered by Werner [34], where a one-to-one equivalence between maximally entangled bases, unitary bases, teleportation schemes, and dense coding schemes has been established. Furthermore, a family of *shift-and-multiply* bases based on Hadamard matrices and Latin squares has been introduced therein.

Limited families of isoentangled bases have been considered in Refs. [20–22], without claims of being complete constructions. Below we demonstrate a method to merge methods from Refs. [21,34], arriving at another family of bases with intermediate entanglement degrees.

First, we focus on a construction from Ref. [34]. Therein, a family of unitary bases based on Hadamard matrices and Latin squares is introduced. Given a $d \times d$ Latin square $\lambda(j,k) : I_d \times I_d \mapsto I_d$ and $j$ (not necessarily distinct) Hadamard matrices, the set of unitary matrices $U^{ij}$ o f dimension $d$ is defined by

$$U^{ij}|k\rangle = (H^j)_{ik}|\lambda(j,k)\rangle, \tag{E3}$$

and they provide an orthogonal unitary basis due to the easily verifiable property:

$$\mathrm{tr}(U^{ij\dagger}U^{i'j'}) = d\delta_{ii'}\delta_{jj'}. \tag{E4}$$

It is also easily verified that vectorized versions

$$U \mapsto |U\rangle = \frac{1}{\sqrt{d}}\sum_{nm} U_{nm}|nm\rangle$$

provide a maximally entangled bases of the $d^2$-dimensional Hilbert space.

We may now replace Hadamard matrices with robust Hadamard matrices considered in Ref. [21], such that $R^j R^{j\dagger} = \mathbb{I}$. The corresponding bistochastic matrix has the structure

$$|R^j|^2 = \begin{pmatrix} a & b & \dots & b \\ b & a & \dots & b \\ \vdots & \vdots & \ddots & \vdots \\ b & b & \dots & a \end{pmatrix}, \tag{E5}$$

with absolute value understood entrywise. Then, *a nonunitary shift-and-multiply basis:*

$$B^{ij}|k\rangle = (R^j)_{ik}|\lambda(j,k)\rangle. \tag{E6}$$

The entire proof from Ref. [34] can be retraced to demonstrate the orthogonality of the resulting states $|B^{ij}\rangle$ and the isoentangled character of the basis down to the specific Schmidt coefficients follows directly from the form of the vectorization map.

Indeed, one can extend the above construction to all unitary $R^j$ such that all rows and columns contain the same amplitudes up to permutation.

It is important to note that the above construction is distinct from the equientangled bases given in Ref. [21], which is already evident on the level of the number of robust Hadamards $R^j$ used in the construction.


[1] C. H. Bennett, G. Brassard, C. Crépeau, R. Jozsa, A. Peres, and W. K. Wootters, Teleporting an unknown quantum state via dual classical and Einstein-Podolsky-Rosen channels, Phys. Rev. Lett. **70**, 1895 (1993).

[2] M. Żukowski, A. Zeilinger, M. A. Horne, and A. K. Ekert, "Event-ready-detectors" Bell experiment via entanglement swapping, Phys. Rev. Lett. **71**, 4287 (1993).

[3] C. H. Bennett and S. J. Wiesner, Communication via one- and two-particle operators on Einstein-Podolsky-Rosen states, Phys. Rev. Lett. **69**, 2881 (1992).

[4] R. Jozsa, M. Koashi, N. Linden, S. Popescu, S. Presnell, D. Shepherd, and A. Winter, Entanglement cost of generalised measurements, Quantum Inf. Comp. **3**, 405 (2003).

[5] E. Chitambar, D. Leung, L. Mančinska, M. Ozols, and A. Winter, Everything you always wanted to know about LOCC (but were afraid to ask), Commun. Math. Phys. **328**, 303 (2014).

[6] E. G. Cavalcanti, R. Chaves, F. Giacomini, and Y.-C. Liang, Fresh perspectives on the foundations of quantum physics, Nat. Rev. Phys. **5**, 323 (2023).

[7] R. D. Sorkin, Impossible measurements on quantum fields, in *Directions in General Relativity: Proceedings of the 1993 International Symposium, Maryland* (Cambridge University Press, Cambridge, 1993), Vol. 2, pp. 293–305.

[8] M. Papageorgiou and D. Fraser, Eliminating the "impossible": Recent progress on local measurement theory for quantum field theory, arXiv:2307.08524.

[9] N. Gisin and F. Del Santo, Towards a measurement theory in QFT: "Impossible" quantum measurements are possible but not ideal, Quantum **8**, 1267 (2024).

[10] M. A. Nielsen and I. Chuang, *Quantum Computation and Quantum Information* (Cambridge University Press, Cambridge, 2002).

[11] I. Hamamura and T. Imamichi, Efficient evaluation of quantum observables using entangled measurements, npj Quantum Inf. **6**, 56 (2020).

[12] J. Niset, A. Acín, U. L. Andersen, N. J. Cerf, R. García-Patrón, M. Navascués, and M. Sabuncu, Superiority of entangled measurements over all local strategies for the estimation of product coherent states, Phys. Rev. Lett. **98**, 260404 (2007).

[13] S. Chen, S. Zhou, A. Seif, and L. Jiang, Quantum advantages for pauli channel estimation, Phys. Rev. A **105**, 032435 (2022).

[14] A. Tavakoli, A. Pozas-Kerstjens, M.-X. Luo, and M.-O. Renou, Bell nonlocality in networks, Rep. Prog. Phys. **85**, 056001 (2022).
[15] S. Wehner, D. Elkouss, and R. Hanson, Quantum internet: A vision for the road ahead, Science **362**, eaam9288 (2018).
[16] A. A. Méthot and V. Scarani, An anomaly of non-locality, Quantum Inf. Comput. **7**, 157 (2007).
[17] N. Brunner, N. Gisin, and V. Scarani, Entanglement and nonlocality are different resources, New J. Phys. **7**, 88 (2005).
[18] A. Tavakoli, N. Gisin, and C. Branciard, Bilocal Bell inequalities violated by the quantum elegant joint measurement, Phys. Rev. Lett. **126**, 220401 (2021).
[19] M. Koniorczyk and V. Bužek, Nonmaximally entangled bases and their application in entanglement purification via swapping, Phys. Rev. A **71**, 032331 (2005).
[20] V. Karimipour and L. Memarzadeh, Equientangled bases in arbitrary dimensions, Phys. Rev. A **73**, 012329 (2006).
[21] G. Rajchel, A. Gąsiorowski, and K. Życzkowski, Robust Hadamard matrices, unistochastic rays in Birkhoff polytope and equi-entangled bases in composite spaces, Math. Comput. Sci. **12**, 473 (2018).
[22] J. Czartowski and K. Życzkowski, Bipartite quantum measurements with optimal single-sided distinguishability, Quantum **5**, 442 (2021).
[23] C.-X. Huang, X.-M. Hu, Y. Guo, C. Zhang, B.-H. Liu, Y.-F. Huang, C.-F. Li, G.-C. Guo, N. Gisin, C. Branciard, and A. Tavakoli, Entanglement swapping and quantum correlations via symmetric joint measurements, Phys. Rev. Lett. **129**, 030502 (2022).
[24] F. Pimpel, M. J. Renner, and A. Tavakoli, Do entangled states correspond to entangled measurements under local transformations? Phys. Rev. A **108**, 022220 (2023).
[25] G. Vidal, Entanglement monotones, J. Mod. Opt. **47**, 355 (2000).
[26] W. K. Wootters, Entanglement of formation of an arbitrary state of two qubits, Phys. Rev. Lett. **80**, 2245 (1998).
[27] P. Rungta, V. Bužek, C. M. Caves, M. Hillery, and G. J. Milburn, Universal state inversion and concurrence in arbitrary dimensions, Phys. Rev. A **64**, 042315 (2001).
[28] N. A. Peters, T.-C. Wei, and P. G. Kwiat, Mixed-state sensitivity of several quantum-information benchmarks, Phys. Rev. A **70**, 052309 (2004).
[29] A. Sanpera, R. Tarrach, and G. Vidal, Local description of quantum inseparability, Phys. Rev. A **58**, 826 (1998).
[30] N. Gisin, Entanglement 25 years after quantum teleportation: Testing joint measurements in quantum networks, Entropy **21**, 325 (2019).
[31] S. Popescu and L. Vaidman, Causality constraints on nonlocal quantum measurements, Phys. Rev. A **49**, 4331 (1994).
[32] M.-O. Renou, E. Bäumer, S. Boreiri, N. Brunner, N. Gisin, and S. Beigi, Genuine quantum nonlocality in the triangle network, Phys. Rev. Lett. **123**, 140401 (2019).
[33] M.-O. Renou, Y. Wang, S. Boreiri, S. Beigi, N. Gisin, and N. Brunner, Limits on correlations in networks for quantum and no-signaling resources, Phys. Rev. Lett. **123**, 070403 (2019).
[34] R. F. Werner, All teleportation and dense coding schemes, J. Phys. A: Math. Gen. **34**, 7081 (2001).